

基于小波分析的交流 CMT 焊接电信号滤波

汪殿龙, 张志洋, 梁志敏, 王 军

(河北科技大学 材料科学与工程学院, 石家庄 050018)

摘 要: 在传统阈值去噪法的基础上提出一种改进阈值去噪算法. 该算法在阈值区间加入处理函数和调节系数, 填补阈值区间内的空白, 从而实现灵活调整信号衰减程度和平滑程度, 提高重构后信号的连续性和逼近程度. 试验利用 coif 小波对交流 CMT 焊接不锈钢电流电压信号进行 3 层分解, 采用改进阈值法对分解后的小波系数进行处理. 结果表明, 通过灵活调整调节系数, 改进算法能够很好地去除交流 CMT 焊接电信号中的高频噪声, 保留有用突变成分和规则脉动信号, 对有用信号的衰减比阈值方法小, 提高了与真实信号的逼近程度, 适用于交流 CMT 焊接电信号的滤波.

关键词: 交流 CMT; 小波变换; 改进阈值法; 信号去噪

中图分类号: TG 403 **文献标识码:** A **文章编号:** 0253-360X(2014)05-0017-04

0 序 言

冷金属过渡(cold metal transfer, CMT)焊接技术是在熔化极气体保护焊短路过渡基础上开发的一种革新技术, 并越来越多地受到研究人员的重视. 交流 CMT 是继直流 CMT 之后一种先进焊接方法. 与直流 CMT 相比, 交流 CMT 拥有更小的热输入、更少的飞溅、更高的焊接速度和熔敷效率以及更好的搭桥能力等优势. 从焊接电信号中提取出电弧电压发生拐点时的突变非平稳信号等特征信息对于研究焊接电弧、焊接工艺等具有重要意义. 但是目前关于交流 CMT 的研究资料非常少, 交流 CMT 焊接工艺比传统的 MIG/MAG 焊接更复杂, 考虑到实验室存在的各种干扰因素会在测试信号上叠加噪声, 当噪声信号的强度较大时, 难以检测原信号的波形, 甚至提取到错误的信息, 不利于对焊接电信号的分析. 因此必须选择合适的滤波方法除去信号中的噪声, 还原出与原始信号最接近的波形信号, 有利于研究人员对信号的分析研究.

1 交流 CMT 焊接电信号特征

CMT 短路过渡与一般短路过渡不同, CMT 控制系统自动监控短路过渡过程, 当有短路信号产生时, 电流降至很低, 电弧几乎熄灭, 同时焊丝回抽, 帮助

熔滴脱落, 从根本上消除了产生飞溅的因素, 整个焊接过程实现“热—冷—热”交替转换. 在这个过程中, 电流和电压同步变化, 交流 CMT 还存在极性转换. 图 1 是一组交流 CMT 电压电流波形.

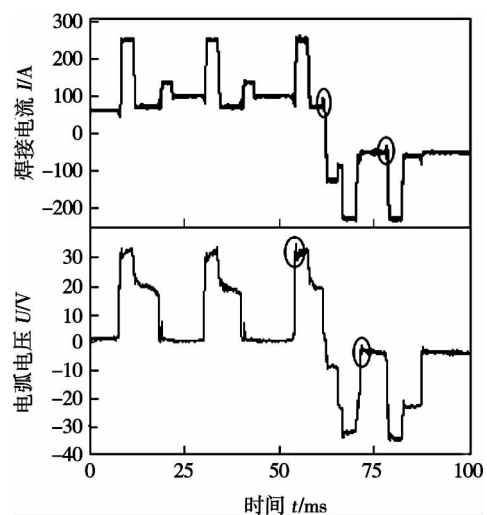


图 1 交流 CMT 电压电流波形

Fig. 1 Waveform of advanced CMT

由图 1 可以看出, 交流 CMT 波形整体上是频率约为 50 ~ 60 Hz 的低频信号, 即熔滴过渡频率; 交流 CMT 电弧交替处于燃弧、短路、回抽、极性转换、短路、回抽、燃弧状态, 在这些状态下会存在尖峰突起, 如图 1 中圈注所示. 频谱范围较宽且幅度较大, 这些突变点产生的原因主要包括: 焊接电源主功率器件引起的开关噪音、短路和燃弧瞬间由焊接电源电感

产生的电压电流尖峰、焊枪回抽焊丝时产生的干扰等,这些突变信号能够反映出焊接电源的性能、焊接工艺优劣及焊接过程的稳定性。此外电流波形上存在很有规律的脉动,频率可达 1.5 kHz,表明此脉动波形并非干扰信号,该信号可能会对熔池、晶粒、焊缝成形或焊接过程产生不可忽视的影响。由以上分析可以看出,交流 CMT 焊接电信号具有非线性、时变的特点,其焊接电流、电弧电压为长时低频成分和短时高频成分组成的时变非平稳信号。因此对于交流 CMT 焊接电信号的处理,要求既能滤除高频干扰信号,又要保留有用的高频及突变信号,一般的低通滤波方法不适合。

传统处理突变信号的方法主要有快速傅里叶变换(fast fourier transform, FFT)技术、FFT 修整技术和卡尔曼滤波技术。FFT 技术和 FFT 修整技术不能用于非平稳信号,而卡尔曼滤波技术用于识别突变信号的一个主要频率,其结果可能会夹杂其它频率的突变。近些年发展起来的小波变换分析方法适用于宽波段信号(包括非平稳信号)变换和分析。在时域上的平移和缩放使得小波变换可以聚焦到高频成分的短时间间隔和低频成分的长时间间隔。该方法已成功应用于图像去噪、微弱信号处理、医学及材料分析等诸多方面^[1-3],在焊接信号处理中的应用也日渐增多,并取得了良好的效果^[4-6]。文中利用小波分析方法对交流 CMT 焊接电信号进行分解和去噪处理。

2 小波滤波方法分析

2.1 小波函数的选取

交流 CMT 焊接电信号去噪过程可采用 Mallat 塔式算法对原始信号进行分解和重构。Mallat 塔式算法是计算离散二进小波变换的快速算法。为了减少小波变换过程的运算量,采用小波变换的卷积定义,即

$$\text{离散平滑逼近: } x_k^{(1)} = x_k^{(0)} \sum h_{0(n-2k)} x_k^{(0)} \quad (1)$$

$$\text{离散细节信号: } d_k^{(1)} = \sum g_{0(n-2k)} x_k^{(0)} \quad (2)$$

式中: $x_k^{(0)}$ 为输入的连续信号; $x_k^{(1)}$ 和 $d_k^{(1)}$ 为经一级分解后得到的概貌信号和细节信号; $h_{0(n-2k)}$ 和 $g_{0(n-2k)}$ 分别为小波分解的低通滤波器和高通滤波器。

利用小波变换的卷积定义,不需要知道尺度函数与小波函数的具体表达式,只由分解与重构滤波器的系数与原始信号进行卷积运算就可以实现信号的分解与重构,这种方法要求小波函数和尺度函数是正交的。

具有正交性的小波基有 haar, db, coif, sym 和 meyr 5 种^[7]。前面的分析表明,交流 CMT 焊接电信号是一种非平稳奇异信号。对于这类信号在信号突变处包含有丰富的信息,通过对信号奇异性的检测,可提取这些信息^[8]。为了能够有效地检测出信号中的奇异点,所选小波基必须具有足够高的消失矩。对比上述 5 种正交小波基,coif 小波基具有较高的消失矩,且具有较长的支撑长度和滤波器长度,适合于交流 CMT 焊接电信号的分解和重构。

2.2 阈值消噪方法分析

阈值消噪法是目前应用较为广泛且有效的去噪方法。常用的阈值处理方法主要有硬阈值法和软阈值法两种。

硬阈值方法表达式为

$$y_n = \begin{cases} x_n, & |x_n| \geq t_0 \\ 0, & |x_n| < t_0 \end{cases} \quad (3)$$

式中: t_0 为阈值; x_n 为输入序列; y_n 为硬阈值处理后的输出序列,其曲线如图 2 所示。

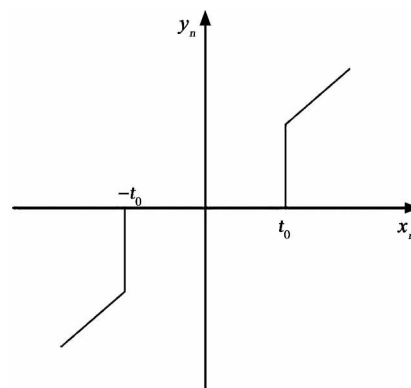


图 2 硬阈值法曲线

Fig. 2 Curve of hard threshold method

从图 2 可以看出,硬阈值法在 $\pm t_0$ 处是不连续的,因而处理后的数据连续性较差,且较大的噪声可能会高于阈值,这样便不能很好地滤除噪声。所以焊接电信号的消噪一般不采用这种方法。

对焊接电信号的处理多采用软阈值法^[9],其表达式为

$$y_n = \begin{cases} \text{sign}(x_n) (|x_n| - t_0), & |x_n| \geq t_0 \\ 0, & |x_n| < t_0 \end{cases} \quad (4)$$

曲线如图 3 所示。由图 3 可以看出,软阈值法在 $\pm t_0$ 处是连续的,处理后的数据比硬阈值法更具有连续性,效果较好。但软阈值法和原系数存在恒定的偏差,处理后的小波系数有一定的衰减,交流 CMT 电信号中有一些很有规律的突变信号,但其幅值相对较小,软阈值法对信号的衰减会使这些信号

削减甚至消失, 影响信号重构后的逼近程度。

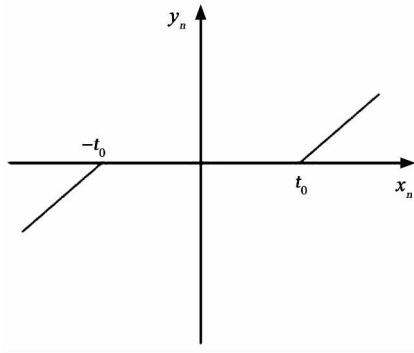


图3 软阈值法曲线

Fig. 3 Curve of soft threshold method

为了提高重构后信号的连续性和逼近程度, 并保留较为微弱的有用突变信号, 提出一种基于软阈值的改进算法, 其表达式为

$$y_n = \begin{cases} \text{sign}(x_n) (t_0 - at_0^3) + x_n, & |x_n| \geq t_0 \\ ax_n^3, & |x_n| < t_0 \end{cases} \quad (5)$$

式中: a 为调节系数, 用来调整 $|x| < t_0$ 范围内的平滑过渡和对信号的衰减程度, 其曲线如图4所示。

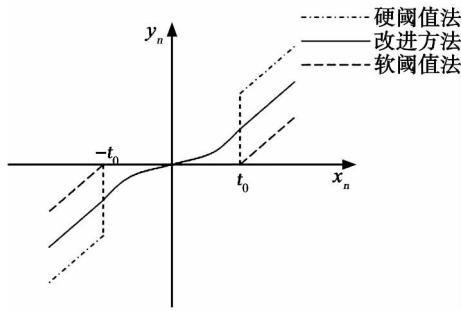


图4 改进算法曲线及其与软、硬阈值法的比较

Fig. 4 Curve of improved threshold method & comparison with the other two methods

由式(5)和图4可以看出, 改进算法综合了硬阈值法和软阈值法的优点, 减小了信号的衰减程度, 并且在 $|x_n| < t_0$ 的范围内添加了一段表达式为 $y = ax^3$ 的函数, 使信号能够平滑过渡, 提高信号的连续性。在交流 CMT 焊接电信号的处理中, 可根据信号中突变信号的具体特点, 灵活调整 a 的值, 使重构后的信号连续且失真最小。当 $a = 0$ 时, 该方法即成为软阈值法。

3 试验结果与分析

通过以上分析, 选用 *coif* 小波基对带有干扰信

号的交流 CMT 焊接电信号进行3层分解, 采用文中提出的改进算法对分解后的小波系数进行处理。阈值 t_0 的计算方法为

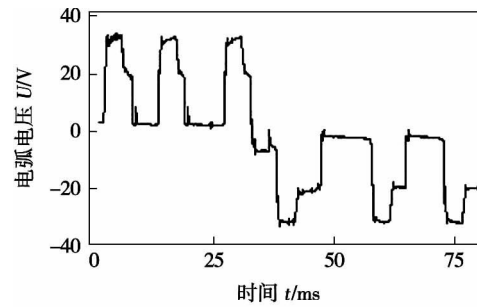
$$t_0 = \hat{\sigma} \sqrt{2 \lg m} \quad (6)$$

$$\hat{\sigma} = \sum_{i=0}^{n-1} |b_i^1| / (0.674 \sqrt{m}) \quad (7)$$

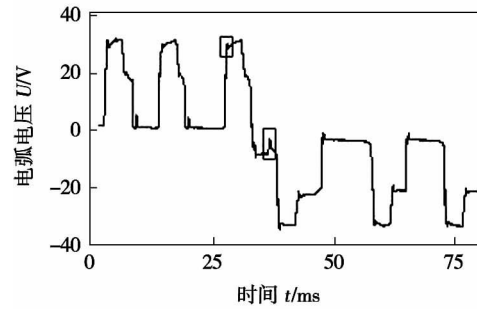
式中: $\hat{\sigma}$ 为噪声强度的近似估计; m 为离散信号的长度; b_i^1 为一级小波变换系数, 调整系数 a 取为 0.05。

试验条件为采用 Fronius CMT Advanced 4000R 型交流 CMT 焊机进行不锈钢堆焊试验, 焊丝直径为 1.0 mm, 设定电弧电压为 25 V, 焊接电流为 200 A, 保护气体为氩气, 气体流量为 15 L/min。

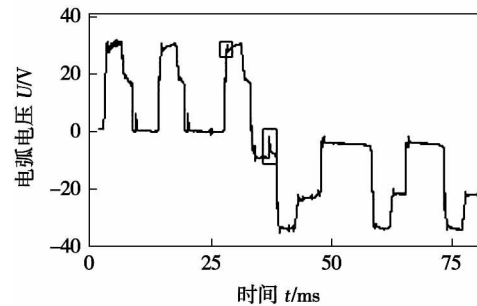
去噪前后的效果对比如图5和图6所示。



(a) 未滤波原始波形



(b) 软阈值法处理后的波形



(c) 改进法处理后的波形

图5 电压波形处理前后对比

Fig. 5 Comparison of original and de-noised arc voltage waveform

由图5和图6可以看出, 经过两种阈值法处理后的信号中噪声明显减少, 原始信号中突变信号和脉动信号均得以保留, 与真实信号的逼近程度很高。

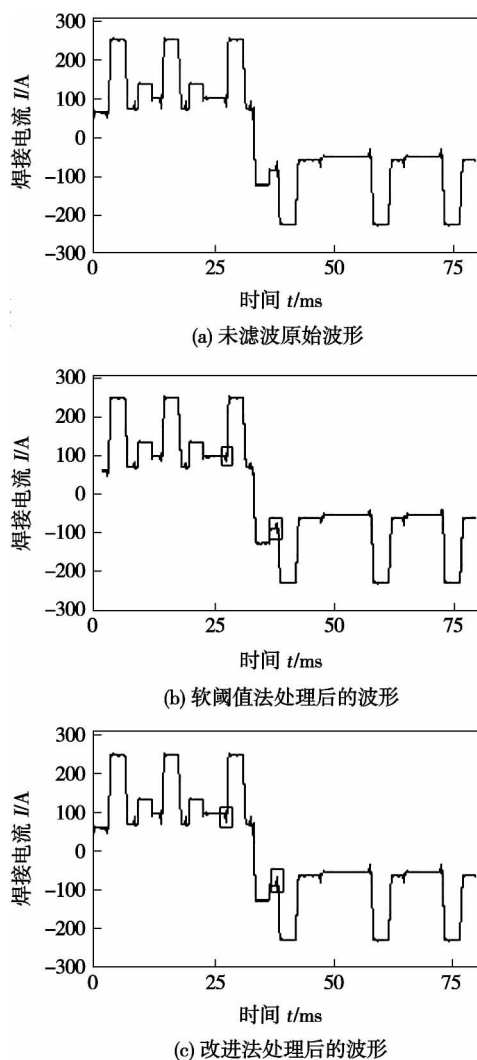


图 6 电流波形处理前后对比

Fig. 6 Comparison of original and de-noised welding current waveform

对比图 6 中方框标示可以看出,软阈值法使波形中突变信号有较大衰减,而改进法中突变信号的幅值与原始信号较为接近,这是改进阈值法的突出优点。

试验结果证明,文中提出的改进算法能够很好地去掉信号中的高频噪声,保留突变成分和规则脉动信号,而对有用信号的衰减要比软阈值方法要小,提高了与真实信号的逼近程度。根据实际情况,灵活调整系数 a 的值,得到了较为理想的结果。

4 结 论

(1) 交流 CMT 焊接电信号由一般的低频成分和一系列规则的、频率大于 1 kHz 的脉动波及高频突变成分组成,频域较宽,传统的快速傅里叶方法和卡尔曼滤波法不适合直接用于交流 CMT 电信号的滤波。

(2) 采用 coif 小波基和卷积算法对交流 CMT

焊接电信号进行分解和重构,并采用文中提出的改进型阈值处理方法对信号进行滤波处理,重构后的信号在除去高频干扰的同时,很好地保留了信号的突变部分,能够还原真实波形的特征,适合于交流 CMT 焊接电信号的滤波。

参考文献:

- [1] 陈天华,韩力群,邢素霞,等. 基于小波变换的心音信号滤波方法研究[J]. 计算机仿真,2012,27(12): 401-405.
Chen Tianhua, Han Liqun, Xing Suxia, et al. Research of de-noising method of heart sound signals based on wavelet transform[J]. Computer Simulation, 2012, 27(12): 401-405.
- [2] 张 婷,郑锡涛. 小波去噪法在复合材料变形测量中的应用[J]. 航空工程进展,2013,4(2): 247-251.
Zhang Ting, Zheng Xitao. Application of wavelet denoising to deformation measurement of composites[J]. Advances in aeronautical science and engineering, 2013, 4(2): 247-251.
- [3] 吴小俊,王怀建. 小波去噪在焊接裂纹声发射信号处理中的应用[J]. 热加工工艺,2011,40(11): 176-181.
Wu Xiaojun, Wang Huaijian. Application of filter noise by wavelet technic in weld crack signal process of acoustic emission [J]. Hot Working Technology, 2011, 40(11): 176-181.
- [4] 薛佳翔,贾林,李海宝,等. 基于 B-spline 小波边缘检测的 CO₂ 熔池和焊缝线检测[J]. 中国焊接,2004,13(2): 137-141.
Xue Jiaxiang, Jia Lin, Li Haibao, et al. Edge detection of molten pool and weld line for CO₂ welding based on B-spline wavelet[J]. China Welding, 2004, 13(2): 137-141.
- [5] 赵辉煌,周德俭,吴兆华,等. 基于小波包变换与自适应阈值的 SMT 焊点图像去噪[J]. 焊接学报,2011,32(11): 73-76.
Zhao Huihuang, Zhou Dejian, Wu Zhaohua, et al. SMT soldering image denoising based on wavelet packet transform and adaptive threshold [J]. Transactions of the China Welding Institution, 2011, 32(11): 73-76.
- [6] Luo Zhen, Shan Ping, Hu Shengsun, et al. Application of the wavelet packet and its energy spectrum to identify Nugget splash during the aluminum alloys spot welding [J]. China Welding, 2003, 12(2): 98-102.
- [7] 汪新凡. 小波基选择及优化[J]. 株洲工学院学报,2003,17(5): 33-35.
Wang Xinfan. Selection and optimization of wavelet base[J]. Journal of Zhuzhou Institute of Technology, 2003, 17(5): 33-35.
- [8] 杨立军,徐立城,张晓因,等. 短路过滤 CO₂ 焊电信号的小波滤波[J]. 焊接学报,2006,27(8): 31-38.
Yang Lijun, Xu Licheng, Zhang Xiaonan, et al. Wavelet filtering of electric signals in short circuit CO₂ welding[J]. Transactions of the China Welding Institution, 2006, 27(8): 31-38.
- [9] 田松亚,顾海涛,付炜亮,等. 基于 DSP 的 CO₂ 焊短路信号的小波检测算法实现[J]. 焊接学报,2010,31(1): 93-96.
Tian Songya, Gu Haitao, Fu Weiliang, et al. Wavelet detection algorithm of short-circuit signal in CO₂ arc welding based on DSP [J]. Transactions of the China Welding Institution, 2010, 31(1): 93-96.

作者简介: 汪殿龙,男,1978 年出生,副教授,博士。主要从事焊接自动化、新型电源变换理论等方面的研究。发表论文 30 余篇。
Email: UC3875@163.com

requirements of underwater wet welding for CCSE36 steel with the water depth of 30 m.

Key words: underwater wet welding; flux-cored wire; CCSE36 steel; mechanical property

Electric signals filtering of AC CMT welding based on wavelet analysis

WANG Dianlong, ZHANG Zhiyang, LIANG Zhimin, WANG Jun (School of Materials Science and Engineering, Hebei University of Science and Technology, Shijiazhuang 050018, China) . pp 17 – 20

Abstract: An improved threshold de-noise algorithm based on the general de-noise threshold algorithm was proposed. A processing function and an adjustment coefficient were added to fill the gap within the threshold range. It is aimed at achieving the flexibility to adjust the degree of attenuation and smoothing and improving the continuity of the reconstructed signal and the degree of approximation of signals. Coif wavelet was used to decompose the electrical signal of stainless steel welding by AC CMT for 3-tier, then the decomposed wavelet coefficients were processed by improved threshold de-noise algorithm. The results showed that by adjusting the adjustment coefficient flexibly, high-frequency noise can be removed well as the useful mutation component and the rule pulsation signals were held through the processing of improved algorithm. The attenuation of the useful signals was lower than that the soft threshold method performed and improved the approximation to the real signals. The improved threshold de-noise algorithm is suitable for filtering of electrical signals of AC CMT.

Key words: AC CMT; wavelet transformation; improved threshold method; filtering for signals

Finite element analysis on friction stir welding of aviation aluminum alloy plate

WANG Hongfeng^{1,2}, WANG Jianli¹, ZUO Dunwen², SONG Weiwei¹, DUAN Xinglin^{1,2} (1. School of Mechanical Electronic & Information Engineering, Huangshan University, Huangshan 245041, China; 2. College of Mechanical and Electrical Engineering, Nanjing University of Aeronautics and Astronautics, Nanjing 210016, China) . pp 21 – 25

Abstract: According to characteristics of friction stir welding, the dynamic heat source model for characteristics of friction stir welding process has been established based on fully considering the friction generating heat between the each parts of the tool and the joining plate, and joining plate friction coefficient with the temperature changing law in the friction stir welding process. By which finite element simulation has been studied for friction stir welding of aviation aluminum alloy sheet. By comparison with simulation results and test results, it could be verified that the established dynamic heat source model and finite element analysis process are reasonable. The simulation results show that the friction stir welding residual tensile stress is concentrated in the joint region, the maximum residual tensile stress appears in the middle of the joint region, and the residual compressive stress appears at the both ends in the joint region and other areas.

Key words: friction stir welding; residual stress; aviation aluminum alloy; heat source model; FEM

Effect of Cr content on deposited metal toughness of weathering steel

XIAO Xiaoming, PENG Yun, YANG Shuai, TIAN Zhiling (State Key Laboratory of Advanced Steel Processes and Products, Central Iron & Steel Research Institute, Beijing 100081, China) . pp 26 – 30

Abstract: The effect of Cr content on microstructure and toughness in deposited metals of weathering steel were investigated by the tensile test, impact test, optical microscope(OM), transmission electron microscopy(TEM), scanning electron microscope(SEM) and electron back-scattered diffraction(EBSD), respectively. The results show that the microstructure consists of granular bainite, acicular ferrite and a few lath bainite for both deposited metals. Good impact toughness is obtained for both deposited metals. Comparing with 1.0% Cr containing deposited metal, the content of granular bainite increases while acicular ferrite decreases of 1.41% Cr containing deposited metal. And the yield strength, tensile strength have improved by 6%, 9%, respectively, but the impact toughness has dropped by 56%. The increasing of the content of M-A constituents and mean grain size, and the decreasing of the number of the large angle boundary of 1.41% Cr containing deposited metal, which cause the rising of the probability of the crack initiation and reducing the resistance to crack propagate, result in its worse toughness.

Key words: weathering steel; deposited metal; Cr content; microstructure; toughness

Effects of electron beam welding with filler wire process on surfacing weld appearance

ZHAO Jian, ZHANG Binggang, LI Xiaopeng, FENG Jicai (State Key Laboratory of Advanced Welding and Joining, Harbin Institute of Technology, Harbin 150001, China) . pp 31 – 34

Abstract: In this paper low carbon steel surfacing layers were formed on 304 stainless steel by electron beam welding with filler wire process to explain the relations between weld appearance and main process parameters. The effects of such welding parameters as electron beam, welding speed, wire feed rate, wire feeding angle and wire feed position on weld appearance were researched. The results showed that the match of weld heat input with wire feed rate was the main factor which determined weld appearance. In the same process, the width of the weld increased while the electron beam increased. Meanwhile, the depth of the weld increased with increasing of the wire feeding angle. In addition, the welding process could be more stable and precise when the front wire feed position was adopted.

Key words: surfacing; electron beam welding; filler wire; surface modification

Brazing of C/C composite and GH99 superalloy Using BNi2 + TiH₂ composite filler powder

TIAN Xiaoyu¹, QI Junlei¹, ZHANG Lixia¹, LIANG Yingchun³, LI Hongwei¹, FENG Jicai^{1,2} (1. State Key Laboratory of Advanced Welding and Joining, Harbin Institute of Technology, Harbin 150001, China; 2. Shandong Provincial Laboratory of Special Welding Technology, Harbin Institute of Technology at Weihai, Weihai 264209, China; 3. School of Mechanical Engineering, Harbin Institute of Technology, Harbin 150001, China) . pp 35 – 38